Genome-wide analysis reveals that Smad3 and JMJD3 HDM co-activate the neural developmental program

Conchi Estarás[1], Naiara Akizu[1,4], Alejandra García[1], Sergi Beltrán[3,5], Xavier de la Cruz[2,6]#, and Marian A. Martínez-Balbás[1]#

[1] Department of Molecular Genomics, Instituto de Biología Molecular de Barcelona (IBMB), Consejo Superior de Investigaciones Científicas (CSIC), 08028 Barcelona, Spain.

[2] Department of Structural Biology. Instituto de Biología Molecular de Barcelona (IBMB-CSIC). Institut Català per la Recerca i Estudis Avançats (ICREA). Parc Científic de Barcelona. 08028 Barcelona, Spain.

[3] Unitat de Bioinformàtica, Centres Científics i Tecnològics - Universitat de Barcelona, 08028 Barcelona, Spain.

[4] Present address: Dept. Neurosciences and Pediatrics. University of California, San Diego. La Jolla, CA 92093-0665, USA.

[5] Present address: Centre Nacional d'Anàlisi Genòmica (CNAG), Parc Científic de Barcelona; 08028 Barcelona, Spain.

[6]Present address: Vall d'Hebron Institute of Research (VHIR), Passeig de la Vall d'Hebron, 119; E-08035 Barcelona, Spain.

#Co-corresponding authors:

E-mail: mmbbmc@ibmb.csic.es; xdmcri@ibmb.csic.es

Tel.: +34 93 4034961; +34 93 4037158

Fax: +34 93 4034979

Running title: JMJD3 regulates TGFβ pathway

Keywords: Histone demethylation/ Epigenetic regulation/ JMJD3/ Smad3/ TGFβ pathway/ Neurogenesis

SUMMARY

Neural development requires crosstalk between signaling pathways and chromatin. In this study, we demonstrate that neurogenesis is promoted by an interplay between the TGFβ pathway and the H3K27me3 histone demethylase (HDM) JMJD3. Genome-wide analysis showed that JMJD3 is targeted to gene promoters by Smad3 in neural stem cells (NSCs) and is essential to activate TGFβ-responsive genes. *In vivo* experiments in chick spinal cord revealed that the generation of neurons promoted by Smad3 is dependent on JMJD3 HDM activity. Overall, these findings indicate that JMJD3 function is required for the TGFβ developmental program to proceed.

INTRODUCTION

Epigenetic mechanisms that regulate access to the genetic material govern cell differentiation and embryonic development. This epigenetic control is mainly mediated by covalent modifications of histones and DNA (Kouzarides, 2007). Recently, histone methylation has received special attention as an essential regulator of gene expression. In particular, methylation of lysine 27 of histone H3 (H3K27me3) has been found to be an important regulator of embryonic development and cell homeostasis (Margueron and Reinberg, 2010; Morey and Helin, 2010). The enzymes responsible for this activity are Enhancer of Zeste Homologs 1 and 2 (EZH1/2) (Cao et al., 2002; Czermin et al., 2002; Kuzmichev et al., 2002). H3K27me3 is recognised by the chromodomain of the polycomb protein that forms part of PRC1 (Cao et al., 2002; Lois et al., 2010). The recruitment of PRC1 leads to final transcriptional repression (Cao et al., 2002), a state which can be reversed by the removal of H3K27me3 marks by Jumonji C (JmjC) domain-containing proteins, JMJD3 and UTX histone demethylases (Agger et al., 2007; De Santa et al., 2007; Lan et al., 2007; Lee et al., 2007). The importance of the balance between methyltransferase and demethylase activity is reflected by the fact that many key developmental promoters are often marked by H3K27me3 (Boyer et al., 2006; Bracken et al., 2006; Lee et al., 2006; Pan et al., 2007). Indeed both UTX and JMJD3 derepress *HOX* genes and a subset of neural and epidermal differentiation genes (Agger et al., 2007; Burgold et al., 2008; Jepsen et al., 2007; Lan et al., 2007; Lee et al., 2007; Sen et al., 2008). In particular, UTX is enriched around the transcription start sites of many HOX genes in primary human fibroblasts, which correlates with a strong decrease in H3K27me3 levels. However in embryonic stem cells (ESCs), in which these genes are repressed, UTX is excluded from the HOX loci (Agger et al., 2007; Lan et al., 2007). In addition, inhibition of a zebrafish UTX homologue or the *Caenorhabditis elegans* JMJD3

orthologue leads to mis-regulation of HOX genes and developmental defects (Agger et al., 2007; Lan et al., 2007). On the other hand, in isolated cortical progenitor cells, SMRT prevents retinoic-neuronal differentiation by repressing the expression of JMJD3, which can activate specific components of the neurogenic program (Jepsen et al., 2007). These findings show an important contribution of JMJD3/UTX during development. However, in spite of the essential role of H3K27me3 and its demethylases during development, we do not know how they respond to developmental signals.

Signaling pathways are essential during development. Specifically, transforming growth factor β (TGFβ) signaling is important for both embryonic development and tissue homeostasis (Moustakas and Heldin, 2009). At the cellular level, TGFβ regulates cell growth, differentiation, adhesion, migration and death in a cell context-dependent manner (Yang and Moses, 2008). On the other hand, alterations in TGFβ signaling lead to congenital malformations, inflammation, and cancer [reviewed by (Gordon and Blobe, 2008; Massague et al., 2005)]. Mechanistically, TGFβ transduces signals from the plasma membrane by interacting with type I and type II receptors, which are serine/threonine kinases. Cytokine binding induces phosphorylation and activation of Smad2 and Smad3 at C-terminal serine residues, while activated Smad2/3 proteins interact with Smad4 to enter the nucleus and regulate gene expression (Feng and Derynck, 2005; Shi and Massague, 2003; Varga and Wrana, 2005). The biological output of TGFβ pathway activation depends on the subset of genes that are regulated in each cellular context (Massague, 2000), which, in turn, varies with each particular combination of cofactors. Specific chromatin modifier enzymes have been associated with activated Smad proteins, such as histone acetyltransferases P/CAF, CBP/p300 or the ATP-dependent remodeling factor Brg1 (Feng and Derynck, 2005; Massague et al., 2005; Xi et al., 2008). In particular, the TGFβ effectors Smad2/3 interact with JMJD3 to de-repress certain loci in

ESCs (Dahle et al., 2010; Kim et al., 2011). Here, we demonstrate by genome-wide analysis and *in vivo* experiments that TGFβ-neural development-associated function requires JMJD3 activity.

The results of the present study show by ChIP-Seq analysis that JMJD3 and Smad3 co-localize at the transcriptional start site (TSS) of TGFβ responsive genes in neural stem cells (NSCs). Moreover, genome wide expression profiling revealed that the neural developmental targets of TGFβ signaling require JMJD3 for proper regulation. Finally, *in vivo* experiments in chick developing spinal cord demonstrated that JMJD3 activity is essential for Smad3-induced neuronal differentiation.

MATERIALS AND METHODS

Cell culture and CoIP assays

Human 293t cells were grown under standard conditions (Blanco-Garcia et al., 2009). Mouse NSCs, provided by Dr K. Helin, were dissected out from cerebral cortex of mouse embryos (E12.5) and cultured in a poly-D-lysine (5μg/ml, 2h 37°C) and laminine (5 μg/ml 37°C, 4 h 37ºC) precoated dishes growing with a media composed by equal parts of DMEM F12 (without Phenol Red, Gibco) and Neural Basal Media (Gibco) containing Penicillin/Streptomycin and Glutamax (1%), N2 and B27 supplements (Gibco), non essential aminoacids (0.1mM), sodium pyruvat (1mM), Hepes (5 mM), Heparin (2 mg/l), bovine serum albumin (25 mg/l) and β mercaptoethanol (0.01 mM). We add fresh recombinant human EGF (R&D systems) and FGF (Invitrogen) to 20 ng/ml and 10 ng/ml final concentrations respectively. NSCs preserve the ability to self-renew and to generate a wide range of differentiated neural cell types (Calloni et al., 2009; Gossrau et al., 2007; Sasaki et al., 2006). TGFβ (Millipore) was used at a final concentration of 5 ng/ml. CoIP experiments were carried out as described (Akizu et al., 2010).

Plasmids and recombinant proteins

Flag-Smad2, Flag-Smad3 and Flag-Smad3S/D cloned into pCIG vector were kindly provided by Dr E. Martí (Garcia-Campmany and Marti, 2007). pCIG-Myc-JMJD3 and pCIG-Myc-JMJD3 DN has been previously described (Akizu et al., 2010). shRNA against chicken JMJD3 was cloned in pShin vector (Kojima et al., 2004). shRNA against mouse JMJD3 is cloned into pLKO.1-puro vector and it was purchased from Sigma [shJMJD3(2837), TRCN0000095265]. GST-Smad3 full-length and GST-Smad3 MH1 domain (1-155) were kindly provided by Dr J. Massagué (Xu et al., 2003). GST-Smad3 MH2 (199-425) and Linker-MH2 (146-425) domains were acquired from Addgene.

Antibodies and reagents

TGFβ was acquired from Millipore (GF111). Antibodies used were anti: mouse Smad3 (Abcam 55480), rabbit ChIP Grade Smad3 (Abcam 28379), rabbit PhosphoSmad3 (Cell Signaling, mAb9520), mouse Flag (Sigma M2), mouse Nestin (BD Bioscience, 611653), mouse b-Tubulin III (Tuj1, Covance MMS-435P), rabbit trimethyl H3K27 (Millipore, 07449), rabbit Sox2 (Invitrogen 48-1400), mouse HuC/D (MP, A21271), rabbit Gfap (Dako, z0334), rabbit Id1 (Santa Cruz, sc488), rabbit ph3 (Upstate 06-570) and mouse Mnr2 (DSHB, 81.5C10). Anti rabbit JMJD3 was kindly given by Dr K. Helin (Agger et al., 2009). Anti mouse Myc antibody was a gift from Dr S. Pons. Anti guinea Pig Lbx1 was kindly provided by Dr E. Martí.

Microarrays analysis

RNA-s from 10^6 non stimulated or TGFβ-stimulated for 2.5 h KD C and KD JMJD3 cells were supplied to the Microarrays Unit of the Centre for Genomic Regulation (CRG) for quality control, quantification, reverse transcription, labeling and hybridization using an Agilent Platform with Whole Mouse Genome microarrays. Triplicates were analyzed for untreated and TGFβ-treated KD C and KD JMJD3 samples. Fold Changes (FCs) between

untreated and the corresponding TGFβ treated samples were calculated applying the AFM tool. The list of JMJD3 dependent TGFβ responsive genes was generated using a two-step protocol. First, we identified the genes putatively sensitive to TGFβ regulation. These were defined as those genes from the KD C with significant values (adjusted p-value ≤ 0.05) for the fold change between gene expression levels in TGFβ treated and untreated cells (this fold change is abbreviated as FC). Second, we used the resulting 2744 gene set to generate the list of candidate genes. This was done by generating two subsets of genes: the subset of genes for which FC remains significant in the KD JMJD3 array (adjusted p-value ≤ 0.05) but showed a lower FC (differences larger than 25% of the corresponding FC in the KD C array); and the subset of genes with non-significant FC (p-value ≥ 0.1) in the KD JMJD3 array experiment. We subsequently put these two subsets together to produce a final list of 781 candidates. Microarray data have been deposited in GEO database under accession No. GSE35361.

ChIP assays

ChIPs from NSCs were carried out using previously described procedures (Frank et al., 2001) with modifications: $3x10^6$ NSCs untreated or treated with TGFβ (5 ng/ml, for the indicated times) were fixed with di (N-succinimidyl) glutarate (DSG) 0.2 mM, 45 min at room temperature followed of FA 1% 20 min. Fixation was stopped by addition of 0.125 mM glycine. The sonication step was performed in a Bioruptor sonicator (12 min, 30 sec ON, 30 sec OFF). ChIP DNA was analyzed by qPCR in a LightCycler 480 PCR system (Roche). ChIPs from electroporated chick cells were essentially performed as described previously (Akizu et al., 2010).

ChIP-Seq procedure

A standard ChIP protocol was used. Before sequencing, ChIP DNA was prepared by simultaneously blunting, repairing and phosphorylating ends according to

manufacturer's instruction (Illumina). The DNA was adenylated at 3' end and recovered by Qiaquick PCR purification kit (Qiagen) according to the manufacturer's recommendations. Adaptors were added by ligation and the ligated fragments were amplified by PCR, resolved in a gel and purified by Qiagen columns. Samples were loaded into individual lanes of flow cell. We generated almost 20 million 36 bp reads for each ChIP sample. Reads were mapped with bowtie (Langmead et al., 2009) to the UCSC (Fujita et al., 2011) *Mus musculus* genome release 9; only sequence reads mapping at unique locations were kept. Peaks were called with MACS (Zhang et al., 2008) on each sample with Input as control. Only one read from each set of duplicates was kept, p-value cutoff for peak detection was set to 1e-4 and PeakSplitter was invoked. The total number of peaks called for Smad3 and for JMJD3 were 98086 and 63154, respectively. PeakAnalyzer (Salmon-Divon et al., 2010) was used to find the closest upstream or downstream refGene Transcription Start Site (TSS). R language and Bioconductor (Gentleman et al., 2004), including packages ShortRead and IRanges (Morgan et al., 2009), were used for further annotation and statistical analysis. ChIP-Seq data have been deposited in GEO database under accession No. GSE36673.

Size exclusion Chromatography

Size exclusion chromatography was performed with whole cell extracts in a Superose-6 10/300 gel filtration column (GE Healthcare) on AKTA purifier system (GE Healthcare).

Purification of recombinant proteins and GST pull down assays

GST pull-downs were performed essentially as described previously (Valls et al., 2003).

Immunoblotting

Immunoblotting was performed with standard procedures and visualized by means of an ECL kit (Amersham).

mRNA extraction and qPCR

mRNA from NSCs was extracted with QIAGEN columns following manufacturer's instructions. mRNA from dissected neural tubes was extracted by TRIZOL (Invitrogen) protocol. qPCR was performed with Sybergreen (Roche) in LC480 Lightcycler (Roche) using the primers in Table S2.

Indirect immunofluorescence

The collected embryos' brachial regions were fixed for 2 h at 4ºC in 4% paraformaldehyde. Indirect immunofluorescence was essentially performed as described previously (Akizu et al., 2010).

***In situ* hybridization**

Whole-mount embryos' RNA *in situ* hybridization was done following standard procedures (Schaeren-Wiemers and Gerfin-Moser, 1993) using ESTbank probes for chick JMJD3, NeuroD1, Ngn2 and Smad3.

GFP+ cell position measurement

Images from electroporated (EP) neural tubes were obtained on Leica SP5 confocal. Maximum projection of 10 sections was generated and used for quantification. Image J software was used to quantify the position of GFP+ cells along the mediolateral axis. **Y** coordinate was used to define the GFP+ cell position respect to the lumen (**Y**=0). First, neural tube mediolateral axis was divided in 4 equal quadrants encompassing the entire Y axis (from lumen to mantle zone). Second, the Y value of each GFP+ cell was defined. Third, GFP+ cells were grouped in one of the quadrants according to their Y values. Finally, the percentage of GFP+ cells in each quadrant was calculated and the average from all quantified sections was represented in the graph (Figure 5D).

Lentiviral transduction

Lentiviral production was performed as described (Rubinson et al., 2003). Viral particles were added to NSCs and infected cells were selected with puromycine (1μg/ml) 24 h later.

Chick *in ovo* electroporation

In ovo electroporation experiments were performed as previously described (Akizu et al., 2010). Total EP DNA was adjusted to 3.5 μg/μl.

Statistical analysis

Quantitative data were expressed as mean and standard deviation (s.d.) of at least three biologically independent experiments. The significance of differences between groups was assessed using the Student's *t*-test (*p<0.05; **p<0.01).

RESULTS

Phosphorylated Smad3 interacts with JMJD3 in NSCs

The TGFβ signaling pathway has recently been reported to have a role in neural development (Garcia-Campmany and Marti, 2007). On the other hand, JMJD3 regulates many developmental and, in particular, key neural promoters (Jepsen et al., 2007). Given this, we wondered whether JMJD3 cooperated in TGFβ-dependent neural development. In order to address this question, we used a suitable neural cell model: NSCs. First, we demonstrated that JMJD3 and the phosphorylated form of Smad3 (Smad3P) co-purified in TGFβ-treated NSC extracts in a gel filtration assay (Figure 1A). We then confirmed that JMJD3 interacts with the Smad3P by co-immunoprecipitation (Co-IP) experiments (Figure 1B). Next, by pull-down assay, we identified that the Smad3 regions responsible for the interaction with JMJD3 are the MH1 and linker domains (Figure 1C, lanes 3 and 5). As these are the least-well conserved domains between Smad2 and Smad3 proteins

(Figure S1A), we tested the specificity of the JMJD3 interaction with Smad proteins. Co-IP assays showed that Smad2 did not interact with JMJD3 (Figure S1B and S1C).

We then wanted to assess whether the Smad3-JMJD3 interaction was biologically relevant for TGFβ function in NSCs. To this end, we established a JMJD3 knockdown (KD) cell line of NSCs that expresses low levels of JMJD3 without affecting Smad3 expression (Figure 1D) and maintaining neural stem cell identity (Figure S2). Then, we analyzed the effects of JMJD3 depletion on the TGFβ response. As shown in Figure 1E, TGFβ treatment of control cells led to a clear decrease in Nestin, a neural progenitor marker. In contrast, TGFβ failed to down-regulate Nestin in JMJD3 KD cells. These findings suggest that changes in neural stem cell identity mediated by TGFβ depend on JMJD3.

TGFβ-induced gene expression profile depends on JMJD3

To explore whether JMJD3 contributes to the TGFβ response, we set out to identify genes co-regulated by TGFβ and JMJD3. For this, we performed a microarray expression experiment with control (C KD) and JMJD3-depleted NSCs (JMJD3 KD) left untreated or treated with TGFβ for 2.5 h (Figure 2A). We confirmed the results of the two microarrays by qPCR of 12 genes selected to cover the whole range of changes in gene expression (Figure S3A). Interestingly, from 2744 TGFβ-responsive genes in control cells (p-value ≤ 0.05: 1493 genes up- and 1251 genes down-regulated, see Figure 2B), 781 targets were not affected to the same extent by TGFβ in JMJD3 depleted cells (see Methods, Figure 2B and Table S1). These correspond to genes regulated by TGFβ in control cells but not efficiently regulated in JMJD3-depleted cells after TGFβ treatment. Of these 781 candidates, 381 showed JMJD3 dependency for transcription activation (Figure 2B, left panel). This was more evident for genes with

larger transcriptional changes upon TGFβ treatment (75% of genes with FC ≥2 were not activated in KD JMJD3 cells, Figure S3B), in agreement with an activating role for JMJD3. Nevertheless, JMJD3 seems to be required to direct or indirectly repress 400 TGFβ down regulated target genes (Figure 2B, right panel). To further characterize the differences between C KD and JMJD3 KD cells in response to TGFβ signaling, we performed an enrichment analysis of Gene Ontology (GO) terms over the 781 JMJD3-dependent genes (Table S1) to identify those biological processes most sensitive to JMJD3 levels in response to TGFβ signaling. The results of this analysis showed that the most significantly enriched GO terms were associated with development ("anatomical structure development", "organ development" and "developmental process" with adjusted p-values of 1.76e-11, 2.75e-11 and 3.86e-11, respectively) (Figure 2C). In addition, other well known TGFβ functions such as apoptosis, or cell proliferation and differentiation were also dependent of JMJD3 (Figure 2C). Overall, this result points to a key role for JMJD3 in the regulation of TGFβ-responsive genes, in particular genes associated to developmental processes. Interestingly, some class II basic helix-loop-helix (bHLH) proneural genes such as neurogenin 2 (*Ngn2*) and inhibitor of DNA binding 3 (*Id3*) (Figure 2C and Table S1), whose activity is essential during neurogenesis, were not fully induced by TGFβ in KD JMJD3 cells.

Smad3 and JMJD3 co-localize on gene promoters

The ability of the TGFβ signaling pathway and JMJD3 to co-regulate gene transcription suggests that Smad3 and JMJD3 bind a subset of common target genes. To investigate this hypothesis, we identified the genome-wide binding sites of Smad3 and JMJD3 in NSCs treated with TGFβ by sequencing DNA fragments of immunoprecipitated chromatin (ChIP-Seq) (Figure 3A). With values normalized to the

input, 98086 and 63154 peaks were detected in ChIP data for Smad3 and JMJD3, respectively. To validate the ChIP-Seq results as well as the specificity of JMJD3 and Smad3 antibodies we performed ChIP followed by qPCR for a representative set of Smad3 and JMJD3 target genes. Specifically, we selected Smad3 and JMJD3 promoter targets corresponding to genes regulated at transcriptional level by Smad3 and JMJD3 (seven up-regulated and seven down-regulated, see Figure S4A and S4B), four promoters of genes not regulated in the microarray experiment (Figure S4A and S4B) and finally, to test the specificity of the antibodies we chose three areas corresponding to intergenic regions occupied only for Smad3 (named as IGR1, IGR2 and IGR3) and three only by JMJD3 (named as IGR4, IGR5 and IGR6) (Figure S4A and S4B). Then, we examined the genomic distribution of the Smad3 and JMJD3 peaks. Our results showed that both Smad3 and JMJD3 peaks are distributed across various genomic regions (Figure S4C), consistent with what has been found in other cell contexts (De Santa et al., 2009; Kim et al., 2011). Importantly, the overlapping regions between Smad3 and JMJD3 are mainly located around the transcription start site (TSS) (Figure S4D and S4E), containing a common peak maximum around -100 bp from the TSS (Figure 3B and 3D). As shown in Figure 3C, 6158 promoters (-1000 to 0 pb from the TSS) were found to be targeted by both Smad3 and JMJD3.

Interestingly, of the 381 genes that showed a JMJD3-dependency for transcriptional activation in the microarray experiment, 215 (56.4%) were bound by Smad3 and JMJD3 (Figure 3E, left panel and Table S1). On the other hand, 192 genes out of those 400 (48%) down regulated in the microarray experiment were also direct targets of Smad3 and JMJD3 (Figure 3E, right panel) suggesting a potential role of JMJD3 in transcriptional repression. Enrichment analysis of GO terms over these 407 (215 up- plus 192 down-regulated) Smad3 and JMJD3 co-regulated direct targets

showed that the most enriched GO terms are again associated with several different aspects of development (Figure 3F).

Taken together, these results indicate that JMJD3 cooperates with Smad3 regulating the expression of genes involved in development.

JMJD3 permanency at promoters is independent on Smad3

To further analyze the mechanism by which TGFβ and JMJD3 cooperate to activate transcription, we studied several genes involved in development and neural function (*Slc16a6, Eomes, Ngn2, Ctgf,* and *Stx3)* from those listed in Table S1. First, we performed a time-course experiment of Smad3 and JMJD3 recruitment at the promoters under study. Results illustrated in Figure 4A and 4B show that soon after activation (30 min), Smad3 and JMJD3 were recruited to the TGFβ-responsive promoters but not to the control gene *Hbb*. Three hours later Smad3 had been displaced, but JMJD3 remained at most promoters (*Slc16a6, Eomes, Ngn2 and Ctgf*) correlating with mRNA accumulation (Figure 4A-B and 4D). Given the known HDM activity of JMJD3, we wondered whether its recruitment resulted in H3K27me3 removal. It was observed that H3K27me3 levels decreased from 3 h after TGFβ treatment in the four methylated promoters (Figure 4C). This change was probably due to JMJD3 because no changes were detected in H3K27me3 levels in JMJD3 KD cells (Figure S5). However, this decrease was slight and not always correlated with mRNA accumulation (Figure 4D). These data suggest that in addition to H3K27me3 activity other JMJD3-dependent functions might be involved in TGFβ-responsive promoter activation.

The simultaneous binding of Smad3 and JMJD3 to common targets 30 min after TGFβ treatment led us to investigate whether Smad3 reduction affects JMJD3 recruitment to promoters. To address this question, we first established a Smad3-depleted

NSC line (Smad3 KD) which express low levels of Smad3 protein without affecting JMJD3 expression (Figure 4E and Figure S2C). Then, we analyzed the binding of Smad3 and JMJD3 in each of the three cell lines (Figure 4F and 4G). We observed that Smad3 binding to the promoters increases upon TGFβ treatment in both the C KD and JMJD3 KD cell lines, while, as expected, the binding was severely reduced in the Smad3 KD cell line (Figure 4F). On the other hand, JMJD3 recruitment to promoters upon TGFβ treatment was only detected in the C KD cell line (Figure 4G).

Taken together, these findings indicate that the TGFβ pathway activates the expression of some target genes through a rapid recruitment of JMJD3 by Smad3 to the corresponding promoters. JMJD3 targeting triggers H3K27 demethylation and subsequent transcriptional initiation, while Smad3 is displaced and no longer required for stable JMJD3 binding. Moreover, the active recruitment of JMJD3 to the non-H3K27-methylated *Ctgf* promoter and the low decrease of H3K27me3 at methylated promoters, suggests that JMJD3 may have an additional role in transcriptional activation, beyond its HDM activity on H3K27me3.

TGFβ-induced neurogenesis in the spinal cord requires JMJD3

The findings described above support the idea that Smad3, together with JMJD3, regulates genes important for neural development (Figure 2C and Figure 3F). Hence, we tested whether JMJD3 cooperates with the TGFβ pathway in an *in vivo* model of neural development, the chick embryo neural tube. Structurally, 3 zones can be distinguished in a transversal section of neural tube; the ventricular zone (VZ) where proliferating progenitors reside, the transition zone (TZ) where neuroblasts exit the cell cycle to initiate differentiation, and the mantle zone (MZ) where final differentiated neurons reside (Figure 5B). We first examined the expression domains of Smad3 and JMJD3 in

developing spinal cord. *In situ* hybridizations (ISH) of transverse sections of Hamburger and Hamilton (HH) stage 24-26 embryos showed that both mRNA were expressed in similar domains: in the dorsal part of the VZ, and in the TZ (Figure 5A and 5B). In addition, Smad3 immunostaining experiments show a similar distribution of active (nuclear) Smad3 (Figure S6). The extended colocalization of Smad3 and JMJD3 along the dorso-ventral axis of the TZ in the neural tube (Figure 5A and 5B) and the previously reported function of Smad3 inducing neuronal differentiation in this model (Garcia-Campmany and Marti, 2007) suggest that Smad3 and JMJD3 could functionally cooperate in developing spinal cord.

To analyze the function of the proteins of interest, we electroporated the recombinant DNAs cloned in a bicistronic vector containing GFP sequence in the neural tube, thus the EP cells were GFP positive (GFP+). It has been previously shown that overexpression of the pseudo-phosphorylated Smad3 (Smad3S/D) in the chick neural tube promotes neuronal differentiation [(Garcia-Campmany and Marti, 2007) and Figure 5C-5J]. The neuronal differentiation phenotype can be monitored in three ways: (i) lateral distribution of GFP-positive cells; (ii) analysis of progenitor markers; and (iii) neuronal differentiation marker expression. Figures 5C and 5D show that Smad3S/D *in ovo* EP cells differentiate earlier and, as a consequence, are mainly in the MZ of the neural tube where fully differentiated neurons are found, in contrast to the even distribution observed for the empty vector EP cells (Figure 5C and 5D). In line with this, Smad3S/D EP cells are excluded from the progenitor zone stained with Sox2 marker (Figure 5E and 5F), and, on the other hand, express high levels of the neuronal differentiation markers HuC/D and Tuj1 (Figure 5G-4J). We then wondered if Smad3 mediated phenotype was related to JMJD3 overexpression, with this purpose we checked JMJD3 mRNA levels upon Smad3

electroporation, but we did not observe any increase in the transcript of the demethylase (Figure S7).

Next we sought to assess the role of endogenous JMJD3 on Smad3-induced neuronal differentiation. With this aim we first cloned an shRNA for chick JMJD3 in a bicistronic vector containing GFP sequence, which efficiently reduces JMJD3 levels (Figure 5K). Then, we electroporated *in ovo* Smad3S/D together with shJMJD3 and analyzed the previously described markers. First, we investigated the distribution of GFP+ cells; In this case, co-EP GFP+ cells failed to migrate to the MZ, in contrast to EP Smad3 S/D cells, indicating that the lack of JMJD3 counteracts Smad3 neurogenic induction (Figure 5C and 5D). Moreover Smad3S/D and shJMJD3 co-EP cells expressed higher levels of Sox2 proliferation marker than Smad3S/D EP cells (percentage of Sox2+/GFP+ cells: empty vector 55.43%, Smad3S/D 6.54%, Smad3S/D together with shRNA-JMJD3 56.26%) (Figure 5E and 5F). In addition, the total number of Sox2+ cells in the EP side was recovered, counteracting the global progenitors reduction promoted by Smad3 (Figure S8A). Furthermore, Smad3-shJMJD3 co-EP cells express less HuC/D and Tuj1 differentiation markers than Smad3S/D EP cells (percentage of HuCD+/GFP+ cells: empty vector 48.96%, Smad3S/D 84.22%, Smad3S/D together with shRNA-JMJD3 41.24%; percentage of Tuj1+/GFP+ cells: empty vector 47.74%, Smad3S/D 85.23%, Smad3S/D together with shRNA-JMJD3 45.33%) (Figure 5G-5J and Figure S8C). And accordingly to the global changes observed in the progenitors population, the increase of differentiated cells (HuCD+ or Tuj1+) promoted by EP of Smad3S/D was impaired in Smad3- shJMJD3 co-EP neural tubes (Figure S8B). To further confirm the cooperation of JMJD3 with active Smad3 to induce neuronal differentiation we performed JMJD3 gain of function experiments. Results in Figure S9 strongly support our previous results by

showing that co EP of Smad3S/P and JMJD3 WT leads to premature and ectopic neuronal differentiation induction.

As the endogenous chick Smad3 is active (Figure S6) we tested the effect of loss of function of JMJD3 on endogenous neuronal differentiation. Electroporation of shJMJD3 alone had a blocking effect on endogenous neuronal differentiation (Figure S10A- S10D), that equally affects dorsal and ventral terminally differentiated neurons (Figure S10E- S10G). These results strongly indicate that JMJD3 is required for Smad3 to induce neuron generation in chick embryo spinal cord.

Next, we wondered about the correlation between the observed phenotypes and the H3K27me3 status of the EP cells. With this aim, we checked the H3K27me3 levels of shJMJD3 and JMJD3 WT EP cells. Results in Figure S11 indicate that even though we could not detect a global increase in the H3K27me3 levels in JMJD3 depleted cells (probably due to technical limitations), we observed a decrease in H3K27me3 signal upon EP of JMJD3 WT. Moreover, this global demethylation promoted by JMJD3 WT electroporation correlates with the dramatic neuronal differentiation observed when Smad3 is co-electroporated with JMJD3 WT (Figure S9). Overall, these results point to an important function of JMJD3 regulating H3K27me3 levels in the neural tube.

Smad3-JMJD3 cooperation requires JMJD3 HDM activity

Based on our previous data, we assessed whether the requirement of JMJD3 for TGFβ-induced neurogenesis in developing spinal cord depends on the HDM activity mediated by the JumonjiC domain of JMJD3. To this end, we used a JMJD3 mutant lacking HDM activity that acts as a dominant negative form of JMJD3 (JMJD3 DN) [(Akizu et al., 2010), Figure S11)]. Figures 5C-5J show that co-electroporation of JMJD3 DN together with Smad3S/D, counteracts Smad3-induced neuronal differentiation,

similar to the effect observed upon EP of Smad3S/D and shJMJD3. Again, electroporation of JMJD3 DN alone blocks endogenous neuronal differentiation (Figure S10A-S10G). These findings demonstrate that the demethylase activity of JMJD3 is essential for Smad3-induced neurogenesis.

NeuroD1 is regulated by Smad3 and JMJD3 HDM activity

Our data using NSCs indicates that Smad3 and JMJD3 cooperate to co-regulate genes important for neural development, among them class II bHLH genes essential for proper neurogenesis (*Ngn2* and *Id3*). bHLH activators show temporal expression sequence during central nervous system development; based on that they can be further divided into neural determination factors such as the proneural genes, *Mash1*, *Ngn1* and *Ngn2*, which are expressed in proliferating neural progenitors at the initiation of neuronal differentiation, and neural differentiation factors, such as *NeuroD1* that is mainly expressed in young post-mitotic neurons undergoing neuronal differentiation (Figure 6A and Figure S12A). In order to investigate the implication of JMJD3 regulating the expression of late bHLH genes we use the developing chicken neural tube where TGFβ signaling induces terminal neural differentiation and patterning specification (Garcia-Campmany and Marti, 2007). We first confirm that the proneural gene *Ngn2* is also a TGFβ target that requires JMJD3 activity to full induction in chick neural tube. To do that, Smad3S/D together with shJMJD3 or JMJD3 DN vector were *in ovo* electroporated, the neural tubes were dissected out 24h later and GFP+ cells sorted by FACS were processed for RNA extraction and analyzed by qPCR (Figure 6B). Results in Figure S12B shows that in chicken neural tube TGFβ also induces *Ngn2* gene expression, moreover this induction was partially blocked by overexpression of JMJD3 DN or shJMJD3 together with the TGFβ effector. Once confirmed that the proneural gene *Ngn2*

is also a TGFβ and JMJD3 target in chicken neural tube, we tested whether Smad3 and JMJD3 promoted neurogenesis by co-regulating late bHLH genes, such as *NeuroD1*. With this aim, 48h EP GFP+ cells were sorted for RNA extraction or ChIP assays (Figure 6B). Figure 6C shows that Smad3S/D electroporation induces *NeuroD1* expression. This induction was severely counteracted by overexpression of JMJD3 DN or shJMJD3 together with the TGFβ effector (Figure 6C). According with *NeuroD1* mRNA expression levels, Co-EP of JMJD3 DN blocked Smad3 induced H3K27 demethylation on the *NeuroD1* promoter (Figure 6D). To check whether this regulation occurs through a direct binding of Smad3 and JMJD3 to *NeuroD1* promoter we electroporated Flag-Smad3 or Myc-JMJD3 and performed ChIP assays in EP cells using Flag or Myc antibodies. Results in Figure 6E and 6F show that Flag-Smad3 binds *NeuroD1* promoter, but this is not the case for Myc-JMJD3. As our previous results in NSCs indicated that JMJD3 requires Smad3 to target promoters (Figure 4G) we electroporated Flag-Smad3 together with Myc-JMJD3 and performed a new Myc-JMJD3 ChIP assay. Results in Figure 6F show that Myc-JMJD3 is recruited to *NeuroD1* promoter in cells co-EP with the TGFβ effector, confirming our previous results that JMJD3 targeting requires Smad3 (Figure 4G).

Overall, our findings highlight an essential role of JMJD3 activity for Smad3-dependent neural vertebrate development through co-regulation of early (*Ngn2)* and late (*NeuroD1)* master genes for neuronal differentiation.

DISCUSSION

Our results demonstrate by genome-wide analysis and experiments in vertebrate embryos that TGFβ response is largely dependent on the Smad3 co-regulator JMJD3.

Although a large number of Smad cofactors have been previously described, how

they provide specificity and plasticity to TGFβ response is still unknown. Recent studies have shown that master transcription factors, such as Oct4 in ESCs, Myod1 in myotubes and PU.1 in pro-B cells select cell-type-specific response to TGFβ signaling (Mullen et al., 2011). Our studies expand this knowledge showing that not a transcription factor, but an epigenetic regulator determines the TGFβ outcome during development. Our results demonstrate that JMJD3 recruitment to Smad3-targeted promoters is essential to trigger the transcriptional activation of TGFβ-responsive genes that are key for development. As we have shown, JMJD3 depletion compromises the transcriptional regulation of developmental genes. Moreover, in the chick neural tube JMJD3 is essential for Smad3-induced neuronal differentiation.

By establishing a molecular link between JMJD3 and TGFβ signaling, our study provides new insight into how a developmental signal is integrated into chromatin to provide the transcriptional plasticity required during development. In addition, our data propose a dynamic H3K27me3 targets behaviour, modulated by signal-dependent targeting, that recruits JMJD3 by DNA sequence-specific transcription factor Smad3 to neuronal genes. The knowledge about how histone demethylases are recruited to the promoter regions is very limited. It has been shown that T-box transcription factors recruit H3K27me3 demethylases to chromatin (Miller et al., 2008; Miller and Weinmann, 2009). Similarly, p53 by interacting with JMJD3 cooperates to control neurogenesis (Sola et al., 2011). Moreover, recent data have revealed that Smad2/3 and Smad1 (Akizu et al., 2010; Dahle et al., 2010; Kim et al., 2011) by interacting with JMJD3 recruit it to some loci. Our data extend these findings showing that (i) JMJD3 specifically interacts with Smad3 and (ii) this association occurs in almost 7000 promoters in NSCs, moreover (iii) we demonstrate that JMJD3 is essential for Smad3 to activate transcription of key neural genes. Finally, our finding reveals that (iiii) TGFβ-dependent neuron generation in chick

embryo spinal cord requires JMJD3 activity (Figure 6G).

The contribution of H3K27me3 demethylation to JMJD3-mediated transcriptional activation is an intriguing question. Our results indicate that H3K27me3 levels decrease 3 h after TGFβ treatment in the methylated promoters (Figure 4C). However, the active recruitment of JMJD3 to the non-H3K27-methylated like *Ctgf* promoter and the low decrease of H3K27me3 at methylated promoters, suggests that in addition to H3K27me3 demethylation other JMJD3-dependent functions might be involved in TGFβ-responsive promoter activation as it has been previously proposed (De Santa et al., 2009; Miller et al., 2010). Finally, our data with JMJD3 DN clearly demonstrate that HDM activity is required to facilitate TGFβ-induced neuronal differentiation as well as to demethylate and activate the key *NeuroD1* promoter. These results open the possibility that other essential factors different than histone H3 might be targeted by JMJD3 HDM activity upon TGFβ signaling activation. This hypothesis would explain the dependency of HDM activity for the JMJD3 function and the lack of correlation with H3K27me3 levels at some analyzed promoters.

In addition to TGFβ pathway, other developmental signaling pathways might also utilize JMJD3 to increase the rate of transcription of responsive genes. In agreement with this idea, our laboratory has recently shown that JMJD3 regulates the BMP pathway by interacting with Smad1 in developing chick spinal cord (Akizu et al., 2010). These data open the possibility that effectors from different signaling pathways may compete with one another for binding and recruitment of JMJD3 to a different set of genes in a particular spatial and temporal order. In line with this, JMJD3 function would depend on the combination of active signaling pathways in each developmental stage.

In summary, this study identifies a new TGFβ signaling-dependent JMJD3 regulatory function demonstrating a role for this demethylase in neural vertebrate

development. Due to the broad range of TGFβ functions in other processes such as cancer, it would now be interesting to investigate the role of TGFβ-dependent JMJD3 transcriptional regulation in other cellular contexts.

ACKNOWLEDGEMENTS

We would like to thank Dr E. Martí, Dr K. Helin, Dr J. Christensen and K. Williams for reagents, technical assistance and helpful discussions. We also thank Dr X. Yang, Dr K. Ge, Dr J. Massagué, Dr J. Seoane, Dr J.C. Reyes and Dr S. Pons for reagents. This study was supported by the grants CSD2006-00049 and BFU2009-11527 to MAMB and BFU2009-11527 and BIO2006-15557 to XC from the Spanish Ministry of Education and Science, 090210 from Fundaciò La Marató de TV3 to MAMB and 200420E578 from the CSIC to XC. CE and NA were recipients of FPU and I3P (I3P-BPD2005) fellowships respectively.

REFERENCES

Agger, K., Cloos, P. A., Christensen, J., Pasini, D., Rose, S., Rappsilber, J., Issaeva, I., Canaani, E., Salcini, A. E. and Helin, K. (2007). UTX and JMJD3 are histone H3K27 demethylases involved in HOX gene regulation and development. *Nature* **449**, 731-734.

Agger, K., Cloos, P. A., Rudkjaer, L., Williams, K., Andersen, G., Christensen, J. and Helin, K. (2009). The H3K27me3 demethylase JMJD3 contributes to the activation of the INK4A-ARF locus in response to oncogene- and stress-induced senescence. *Genes Dev.* **23**, 1171-1176.

Akizu, N., Estaras, C., Guerrero, L., Marti, E. and Martinez-Balbas, M. A. (2010). H3K27me3 regulates BMP activity in developing spinal cord. *Development* **137**, 2915-2925.

Blanco-Garcia, N., Asensio-Juan, E., de la Cruz, X. and Martinez-Balbas, M. A. (2009). Autoacetylation regulates P/CAF nuclear localization. *J. Biol. Chem.* **284**, 1343-1352.

Boyer, L. A., Plath, K., Zeitlinger, J., Brambrink, T., Medeiros, L. A., Lee, T. I., Levine, S. S., Wernig, M., Tajonar, A., Ray, M. K. et al. (2006). Polycomb complexes repress developmental regulators in murine embryonic stem cells. *Nature* **441**, 349-353.

Bracken, A. P., Dietrich, N., Pasini, D., Hansen, K. H. and Helin, K. (2006). Genome-wide mapping of Polycomb target genes unravels their roles in cell fate transitions. *Genes Dev.* **20**, 1123-1136.
Burgold, T., Spreafico, F., De Santa, F., Totaro, M. G., Prosperini, E., Natoli, G. and Testa, G. (2008). The histone H3 lysine 27-specific demethylase Jmjd3 is required for neural commitment. *PLoS One* **3**, e3034.
Calloni, G. W., Le Douarin, N. M. and Dupin, E. (2009). High frequency of cephalic neural crest cells shows coexistence of neurogenic, melanogenic, and osteogenic differentiation capacities. *Proc. Natl. Acad. Sci. U S A* **106**, 8947-8952.
Cao, R., Wang, L., Wang, H., Xia, L., Erdjument-Bromage, H., Tempst, P., Jones, R. S. and Zhang, Y. (2002). Role of histone H3 lysine 27 methylation in Polycomb-group silencing. *Science* **298**, 1039-1043.
Czermin, B., Melfi, R., McCabe, D., Seitz, V., Imhof, A. and Pirrotta, V. (2002). Drosophila enhancer of Zeste/ESC complexes have a histone H3 methyltransferase activity that marks chromosomal Polycomb sites. *Cell* **111**, 185-196.
Dahle, O., Kumar, A. and Kuehn, M. R. (2010). Nodal signaling recruits the histone demethylase Jmjd3 to counteract polycomb-mediated repression at target genes. *Sci. Signal* **3**, ra48.
De Santa, F., Narang, V., Yap, Z. H., Tusi, B. K., Burgold, T., Austenaa, L., Bucci, G., Caganova, M., Notarbartolo, S., Casola, S. et al. (2009). Jmjd3 contributes to the control of gene expression in LPS-activated macrophages. *EMBO J.* **28**, 3341-3352.
De Santa, F., Totaro, M. G., Prosperini, E., Notarbartolo, S., Testa, G. and Natoli, G. (2007). The histone H3 lysine-27 demethylase Jmjd3 links inflammation to inhibition of polycomb-mediated gene silencing. *Cell* **130**, 1083-1094.
Feng, X. H. and Derynck, R. (2005). Specificity and versatility in tgf-beta signaling through Smads. *Annu. Rev. Cell. Dev. Biol.* **21**, 659-693.
Frank, S. R., Schroeder, M., Fernandez, P., Taubert, S. and Amati, B. (2001). Binding of c-Myc to chromatin mediates mitogen-induced acetylation of histone H4 and gene activation. *Genes Dev.* **15**, 2069-2082.
Fujita, P. A., Rhead, B., Zweig, A. S., Hinrichs, A. S., Karolchik, D., Cline, M. S., Goldman, M., Barber, G. P., Clawson, H., Coelho, A. et al. (2011). The UCSC Genome Browser database: update 2011. *Nucleic Acids Res.* **39**, D876-882.
Garcia-Campmany, L. and Marti, E. (2007). The TGFbeta intracellular effector Smad3 regulates neuronal differentiation and cell fate specification in the developing spinal cord. *Development* **134**, 65-75.
Gentleman, R. C., Carey, V. J., Bates, D. M., Bolstad, B., Dettling, M., Dudoit, S., Ellis, B., Gautier, L., Ge, Y., Gentry, J. et al. (2004). Bioconductor: open software development for computational biology and bioinformatics. *Genome Biol.* **5**, R80.
Gordon, K. J. and Blobe, G. C. (2008). Role of transforming growth factor-beta superfamily signaling pathways in human disease. *Biochim. Biophys. Acta* **1782**, 197-228.
Gossrau, G., Thiele, J., Konang, R., Schmandt, T. and Brustle, O. (2007). Bone morphogenetic protein-mediated modulation of lineage diversification during neural differentiation of embryonic stem cells. *Stem Cells* **25**, 939-949.
Jepsen, K., Solum, D., Zhou, T., McEvilly, R. J., Kim, H. J., Glass, C. K., Hermanson, O. and Rosenfeld, M. G. (2007). SMRT-mediated repression of an H3K27 demethylase in progression from neural stem cell to neuron. *Nature* **450**, 415-419.

Kim, S. W., Yoon, S. J., Chuong, E., Oyolu, C., Wills, A. E., Gupta, R. and Baker, J. (2011). Chromatin and transcriptional signatures for Nodal signaling during endoderm formation in hESCs. *Dev. Biol.* **357**, 492-504.
Kojima, S., Vignjevic, D. and Borisy, G. G. (2004). Improved silencing vector co-expressing GFP and small hairpin RNA. *Biotechniques* **36**, 74-79.
Kouzarides, T. (2007). Chromatin modifications and their function. *Cell* **128**, 693-705.
Kuzmichev, A., Nishioka, K., Erdjument-Bromage, H., Tempst, P. and Reinberg, D. (2002). Histone methyltransferase activity associated with a human multiprotein complex containing the Enhancer of Zeste protein. *Genes Dev.* **16**, 2893-2905.
Lan, F., Bayliss, P. E., Rinn, J. L., Whetstine, J. R., Wang, J. K., Chen, S., Iwase, S., Alpatov, R., Issaeva, I., Canaani, E. et al. (2007). A histone H3 lysine 27 demethylase regulates animal posterior development. *Nature* **449**, 689-694.
Langmead, B., Trapnell, C., Pop, M. and Salzberg, S. L. (2009). Ultrafast and memory-efficient alignment of short DNA sequences to the human genome. *Genome Biol.* **10**, R25.
Lee, M. G., Villa, R., Trojer, P., Norman, J., Yan, K. P., Reinberg, D., Di Croce, L. and Shiekhattar, R. (2007). Demethylation of H3K27 regulates polycomb recruitment and H2A ubiquitination. *Science* **318**, 447-450.
Lee, M. G., Wynder, C., Bochar, D. A., Hakimi, M. A., Cooch, N. and Shiekhattar, R. (2006). Functional interplay between histone demethylase and deacetylase enzymes. *Mol. Cell. Biol.* **26**, 6395-6402.
Lois, S., Akizu, N., de Xaxars, G. M., Vazquez, I., Martinez-Balbas, M. and de la Cruz, X. (2010). Characterization of structural variability sheds light on the specificity determinants of the interaction between effector domains and histone tails. *Epigenetics* **5**, 137-148.
Margueron, R. and Reinberg, D. (2010). Chromatin structure and the inheritance of epigenetic information. *Nat. Rev. Genet.* **11**, 285-296.
Massague, J. (2000). How cells read TGF-beta signals. *Nat. Rev. Mol. Cell. Biol.* **1**, 169-178.
Massague, J., Seoane, J. and Wotton, D. (2005). Smad transcription factors. *Genes Dev.* **19**, 2783-2810.
Miller, S. A., Huang, A. C., Miazgowicz, M. M., Brassil, M. M. and Weinmann, A. S. (2008). Coordinated but physically separable interaction with H3K27-demethylase and H3K4-methyltransferase activities are required for T-box protein-mediated activation of developmental gene expression. *Genes Dev.* **22**, 2980-2993.
Miller, S. A., Mohn, S. E. and Weinmann, A. S. (2010). Jmjd3 and UTX play a demethylase-independent role in chromatin remodeling to regulate T-box family member-dependent gene expression. *Mol. Cell* **40**, 594-605.
Miller, S. A. and Weinmann, A. S. (2009). An essential interaction between T-box proteins and histone-modifying enzymes. *Epigenetics* **4**, 85-88.
Morey, L. and Helin, K. (2010). Polycomb group protein-mediated repression of transcription. *Trends Biochem. Sci.* **35**, 323-332.
Morgan, M., Anders, S., Lawrence, M., Aboyoun, P., Pages, H. and Gentleman, R. (2009). ShortRead: a bioconductor package for input, quality assessment and exploration of high-throughput sequence data. *Bioinformatics* **25**, 2607-2608.

Moustakas, A. and Heldin, C. H. (2009). The regulation of TGFbeta signal transduction. *Development* **136**, 3699-3714.
Mullen, A. C., Orlando, D. A., Newman, J. J., Loven, J., Kumar, R. M., Bilodeau, S., Reddy, J., Guenther, M. G., DeKoter, R. P. and Young, R. A. (2011). Master transcription factors determine cell-type-specific responses to TGF-beta signaling. *Cell* **147**, 565-576.
Pan, G., Tian, S., Nie, J., Yang, C., Ruotti, V., Wei, H., Jonsdottir, G. A., Stewart, R. and Thomson, J. A. (2007). Whole-genome analysis of histone H3 lysine 4 and lysine 27 methylation in human embryonic stem cells. *Cell Stem Cell* **1**, 299-312.
Rubinson, D. A., Dillon, C. P., Kwiatkowski, A. V., Sievers, C., Yang, L., Kopinja, J., Rooney, D. L., Zhang, M., Ihrig, M. M., McManus, M. T. et al. (2003). A lentivirus-based system to functionally silence genes in primary mammalian cells, stem cells and transgenic mice by RNA interference. *Nat. Genet.* **33**, 401-406.
Salmon-Divon, M., Dvinge, H., Tammoja, K. and Bertone, P. (2010). PeakAnalyzer: genome-wide annotation of chromatin binding and modification loci. *BMC Bioinformatics* **11**, 415.
Sasaki, T., Ito, Y., Bringas, P., Jr., Chou, S., Urata, M. M., Slavkin, H. and Chai, Y. (2006). TGFbeta-mediated FGF signaling is crucial for regulating cranial neural crest cell proliferation during frontal bone development. *Development* **133**, 371-381.
Schaeren-Wiemers, N. and Gerfin-Moser, A. (1993). A single protocol to detect transcripts of various types and expression levels in neural tissue and cultured cells: in situ hybridization using digoxigenin-labelled cRNA probes. *Histochemistry* **100**, 431-440.
Sen, G. L., Webster, D. E., Barragan, D. I., Chang, H. Y. and Khavari, P. A. (2008). Control of differentiation in a self-renewing mammalian tissue by the histone demethylase JMJD3. *Genes Dev.* **22**, 1865-1870.
Shi, Y. and Massague, J. (2003). Mechanisms of TGF-beta signaling from cell membrane to the nucleus. *Cell* **113**, 685-700.
Sola, S., Xavier, J. M., Santos, D. M., Aranha, M. M., Morgado, A. L., Jepsen, K. and Rodrigues, C. M. (2011). p53 interaction with JMJD3 results in its nuclear distribution during mouse neural stem cell differentiation. *PLoS One* **6**, e18421.
Valls, E., de la Cruz, X. and Martinez-Balbas, M. A. (2003). The SV40 T antigen modulates CBP histone acetyltransferase activity. *Nucleic Acids Res.* **31**, 3114-3122.
Varga, A. C. and Wrana, J. L. (2005). The disparate role of BMP in stem cell biology. *Oncogene* **24**, 5713-5721.
Xi, Q., He, W., Zhang, X. H., Le, H. V. and Massague, J. (2008). Genome-wide impact of the BRG1 SWI/SNF chromatin remodeler on the transforming growth factor beta transcriptional program. *J. Biol. Chem.* **283**, 1146-1155.
Xu, L., Alarcon, C., Col, S. and Massague, J. (2003). Distinct domain utilization by Smad3 and Smad4 for nucleoporin interaction and nuclear import. *J. Biol. Chem.* **278**, 42569-42577.
Yang, L. and Moses, H. L. (2008). Transforming growth factor beta: tumor suppressor or promoter? Are host immune cells the answer? *Cancer Res.* **68**, 9107-9111.
Zhang, Y., Liu, T., Meyer, C. A., Eeckhoute, J., Johnson, D. S., Bernstein, B. E., Nusbaum, C., Myers, R. M., Brown, M., Li, W. et al. (2008). Model-based analysis of ChIP-Seq (MACS). *Genome Biol.* **9**, R137.

FIGURE LEGENDS

Figure 1. Endogenous Smad3 and JMJD3 interact in NSCs

(A) Size-exclusion chromatography of NSC lysate showing co-elution of Smad3P and JMJD3 and the presence of Smad3 in the lower weight fractions.

(B) Co-IP of mouse NSCs lysate using anti-Smad3P antibody or unrelated IgGs in the presence or absence of TGFβ for 30 min.

(C) Upper panel shows schematic representation of GST-Smad3 fragments: full length (FL), MH1 (1-155 aa), MH2 (199-425 aa) and linker domains that also contains MH2 (146-425 aa). Pull-down assay using GST-Smad3 fusion proteins and 293t cell extracts overexpressing Myc-JMJD3. Ponceau staining of GST-Smad3 proteins (lower panel).

(D) Immunoblot from control knockdown (C KD) and JMJD3 knockdown (JMJD3 KD) cell extracts using the indicated antibodies.

(E) Immunoblot showing Nestin expression prior to and after TGFβ treatment for the indicated times in C KD and JMJD3 KD cells. Nestin levels (relative to Actin) were quantified by using the Image J software (graph on the right).

Input (In) corresponds to 1% of the protein present in the whole cell extract.

Figure 2. TGFβ and JMJD3 regulate common target genes

(A) Schematic representation of microarray analysis design.

(B) Diagrams depict the number of TGFβ-responsive genes that need JMJD3 to be efficiently up (on the left) or down regulated (on the right).

(C) GO analysis of the TGFβ-responsive genes dependent on JMJD3.

Figure 3. Smad3 and JMJD3 co-localize on gene promoters

(A) ChIP-Seq experimental procedure.

(B) Distribution of the distance of Smad3 (blue) and JMJD3 (red) peaks from the TSS.

(C) Venn diagram showing promoters (-1000 to TSS) co-bound by Smad3 and JMJD3.

(D) Representation based on BED files obtained for Smad3 and JMJD3 (see legend) binding sites on *Ngn2* and *Slc16a6* promoters.

(E) Venn diagrams showing genes co-bound by Smad3 and JMJD3 (±1000pb from TSS) that are transcriptionally up regulated (on the left) or down regulated by TGFβ and JMJD3 (on the right).

(F) GO analysis of genes co-bound by Smad3 and JMJD3 that are transcriptionally regulated by TGFβ and JMJD3 (407 targets; 215 up- plus 192 down-regulated).

Figure 4. Smad3 recruits JMJD3 to promoters in response to TGFβ

(A-D) ChIPs [of Smad3 (A), JMJD3 (B) and H3K27me3 (C)] and mRNA levels (D) analyzed by qPCR were performed in NSCs left untreated (0 h) or treated with TGFβ (30 min, 3 h or 6 h). Graphs on the right represent the mean levels at the analyzed promoters.

(E) Immunoblot from C KD and Smad3 KD cell extracts using the indicated antibodies.

(F-G) ChIPs of Smad3 (F) and JMJD3 (G) analyzed by qPCR at the indicated promoters were performed prior to and after TGFβ treatment (30 min) in C KD, JMJD3 KD and Smad3 KD NSC lines (see coloured squares in legend).

ChIP results are presented as fold enrichment over a region negative for Smad3 and JMJD binding (G6pd2 gene, see Table S2). Hbb is an additional negative control represented in the graph. Three biological replicates were used in each ChIP experiment.

Figure 5. Smad3 and JMJD3 cooperate to induce neuronal differentiation in chick spinal cord

(A) Smad3 and JMJD3 mRNA ISHs in HH25-26 embryo spinal cord.

(B) Schematic representation of Smad3 and JMJD3 expression domains shown in (A).

(C, E, G and I) HH12 embryos were electroporated *in ovo* with the DNAs (cloned into a bicistronic vector containing GFP) indicated in the vertical boxes and processed (48 h

PE) for the indicated immunostaining. The right side corresponds to the electroporated side (GFP positive).

(D) Quantification of the lateral distribution of GFP+ cells from the lumen to the mantle zone of the neural tube (see Methods).

(F, H, J) Graphs showing the percentage of electroporated cells (GFP+) positive for Sox2, HuCD and Tuj1 respectively. Data are the mean of n=30 sections (from 4-6 embryos).

(K) JMJD3 mRNA levels were determined by qPCR from sorted EP neural tube cells (GFP+) with the empty vector (E. vector) or shRNA of JMJD3 containing vector (shJMJD3) for 48 h.

Figure 6*. Neuro D1* is a target of Smad3 and JMJD3 in the neural tube

(A) Schematic representation of bHLH genes expression along neurogenesis.

(B) Schematic representation of chick embryo RNA extraction and ChIP procedures.

(C) *NeuroD1* mRNA levels from EP neural tube cells (GFP+) with the indicated DNAs were determined by qPCR.

(D-F) ChIPs analyzed by qPCR from EP neural tube cells (GFP+) with DNAs indicated on the x-axis of the graphs using H3K27me3 (C) , Flag (D) and Myc (E) antibodies at the *NeuroD1* promoter. Results are represented as fold enrichment over negative binding regions for Smad3 and JMJD3. *Tll* promoter was used as negative control for Smad3 and JMJD3 binding and *Hes5* promoter as negative control for H3K27me3. Three biological replicates were used in each experiment.

(G) Schematic diagram summarizing our results. In the non EP side of the neural tube Smad3 drives neuronal differentiation activating the expression of neuronal genes in the TZ (such as *NeuroD1*) together with JMJD3. In the side EP with loss of function (LOF)

of JMJD3, Smad3 is not able to efficiently activate proneural genes leading a reduction in the number of differentiated neurons (see HuC/D marker in red).

FIGURE 1

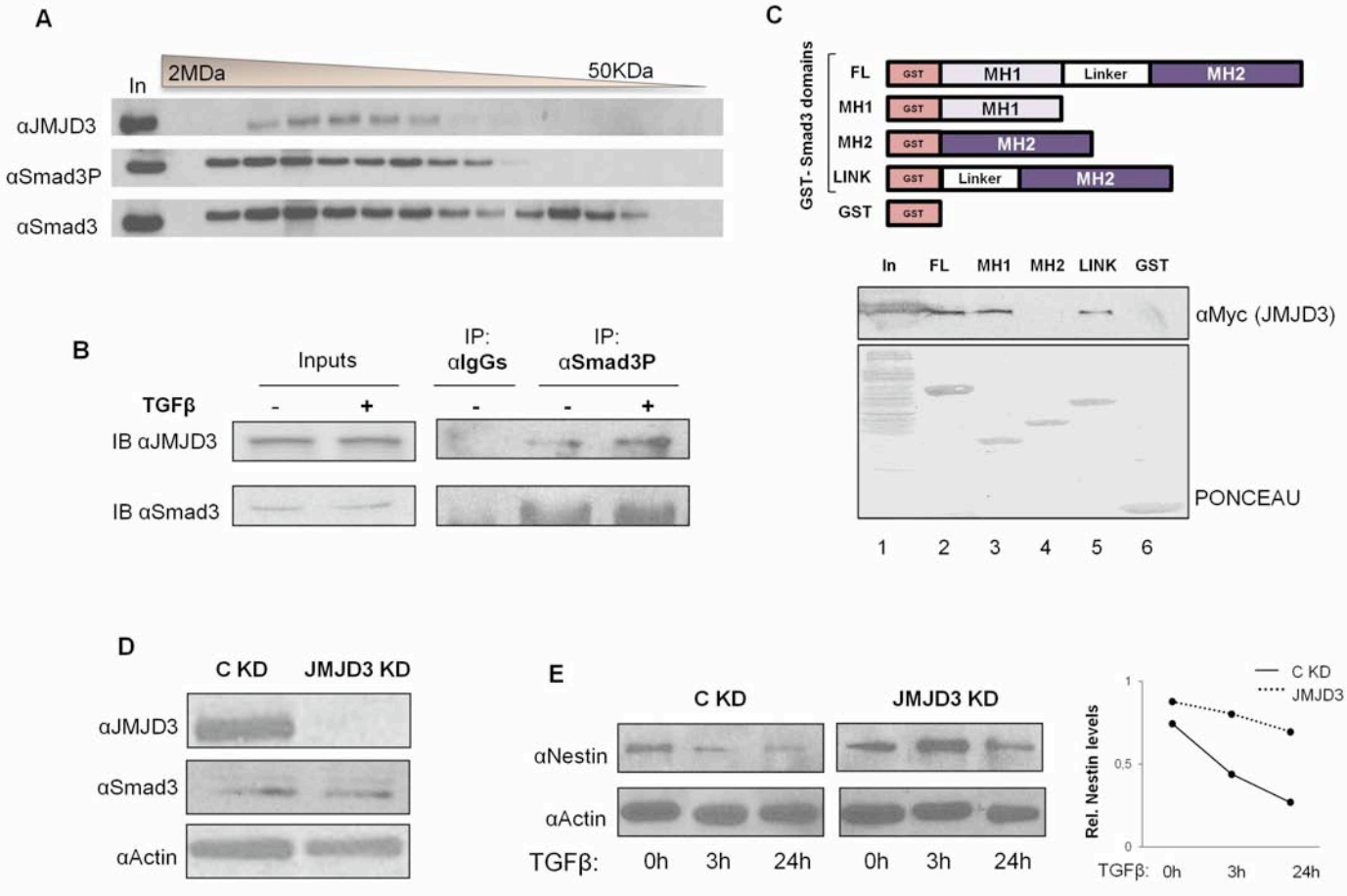
A
In
2MDa
50KDa
αJMJD3
αSmad3P
αSmad3
B
Inputs
IP: αIgGs
IP: αSmad3P
TGFβ
-
+
-
-
+
IB αJMJD3
IB αSmad3
C
GST- Smad3 domains
FL
MH1
MH2
LINK
GST
Linker
In
FL
MH1
MH2
LINK
GST
αMyc (JMJD3)
PONCEAU
1
2
3
4
5
6
D
C KD
JMJD3 KD
αJMJD3
αSmad3
αActin
E
C KD
JMJD3 KD
αNestin
αActin
TGFβ:
0h
3h
24h
0h
3h
24h
Rel. Nestin levels
1
0,5
0
C KD
JMJD3 KD
TGFβ:
0h
3h
24h

FIGURE 2

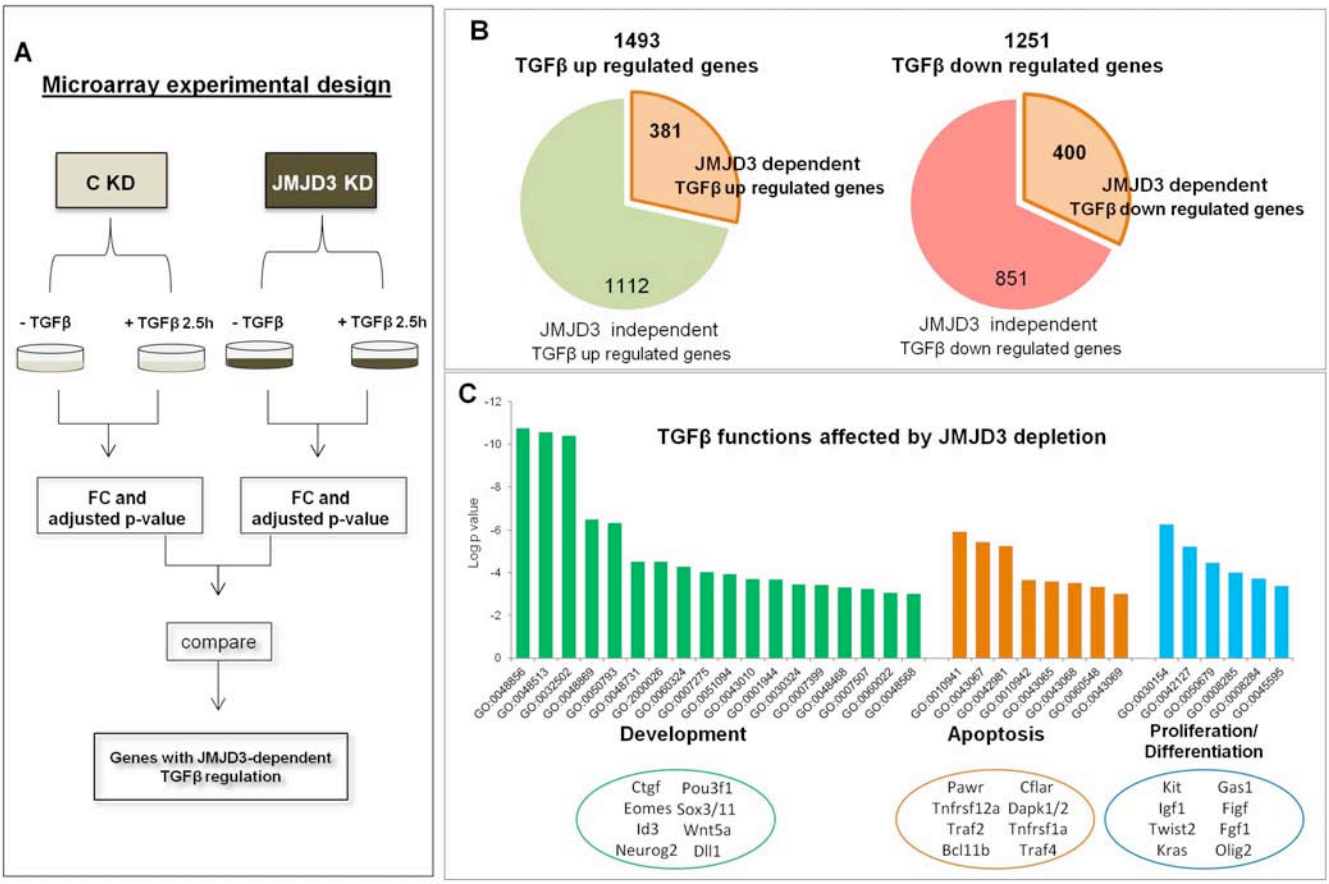
A
Microarray experimental design
C KD
JMJD3 KD
- TGFβ
+ TGFβ 2.5h
- TGFβ
+ TGFβ 2.5h
FC and adjusted p-value
FC and adjusted p-value
compare
Genes with JMJD3-dependent TGFβ regulation
B
1493
TGFβ up regulated genes
381
JMJD3 dependent TGFβ up regulated genes
1112
JMJD3 independent TGFβ up regulated genes
1251
TGFβ down regulated genes
400
JMJD3 dependent TGFβ down regulated genes
851
JMJD3 independent TGFβ down regulated genes
C
TGFβ functions affected by JMJD3 depletion
Log p value
Development
Apoptosis
Proliferation/ Differentiation
Ctgf Pou3f1
Eomes Sox3/11
Id3 Wnt5a
Neurog2 Dll1
Pawr Cflar
Tnfrsf12a Dapk1/2
Traf2 Tnfrsf1a
Bcl11b Traf4
Kit Gas1
Igf1 Figf
Twist2 Fgf1
Kras Olig2

FIGURE 3

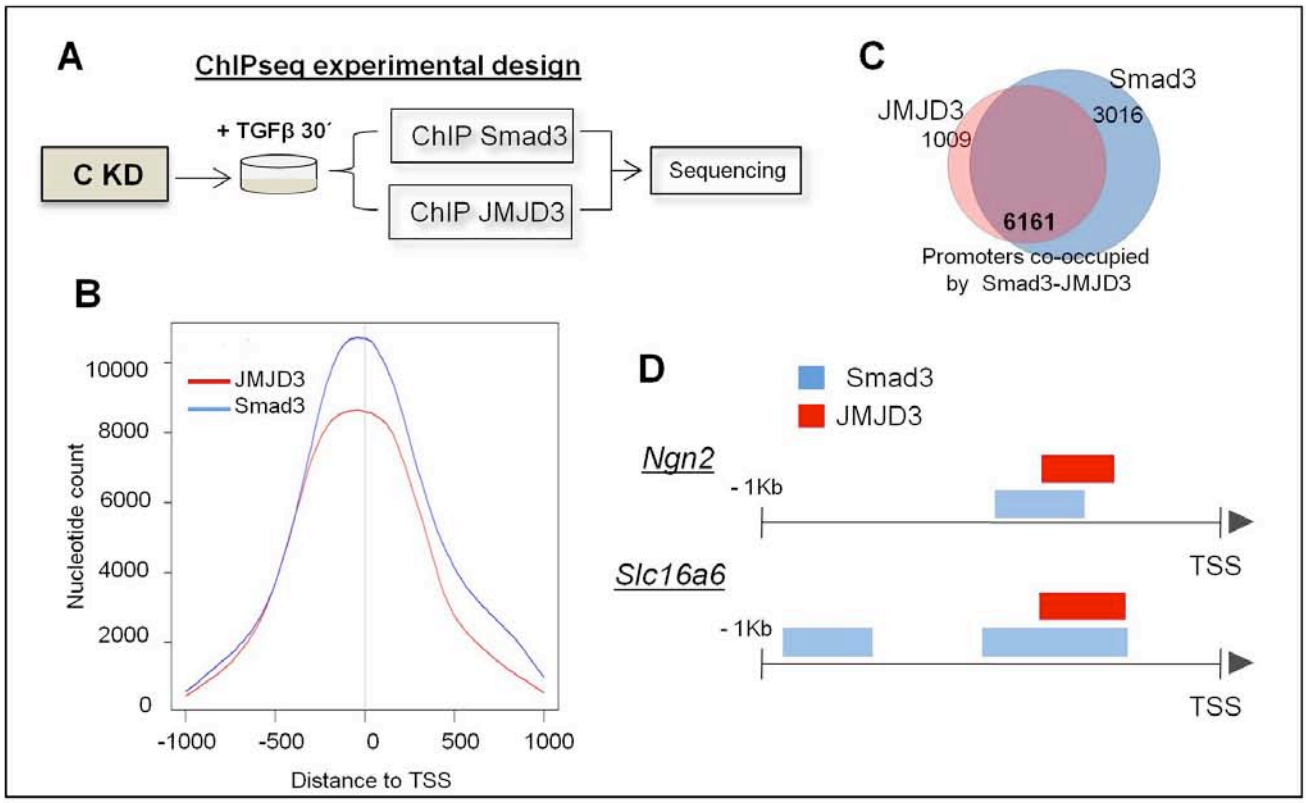
A
ChIPseq experimental design
C KD
+ TGFβ 30´
ChIP Smad3
ChIP JMJD3
Sequencing
C
Smad3
JMJD3
1009
3016
6161
Promoters co-occupied
by Smad3-JMJD3
B
JMJD3
Smad3
Nucleotide count
10000
8000
6000
4000
2000
0
-1000
-500
0
500
1000
Distance to TSS
D
Smad3
JMJD3
Ngn2
- 1Kb
TSS
Slc16a6
- 1Kb
TSS

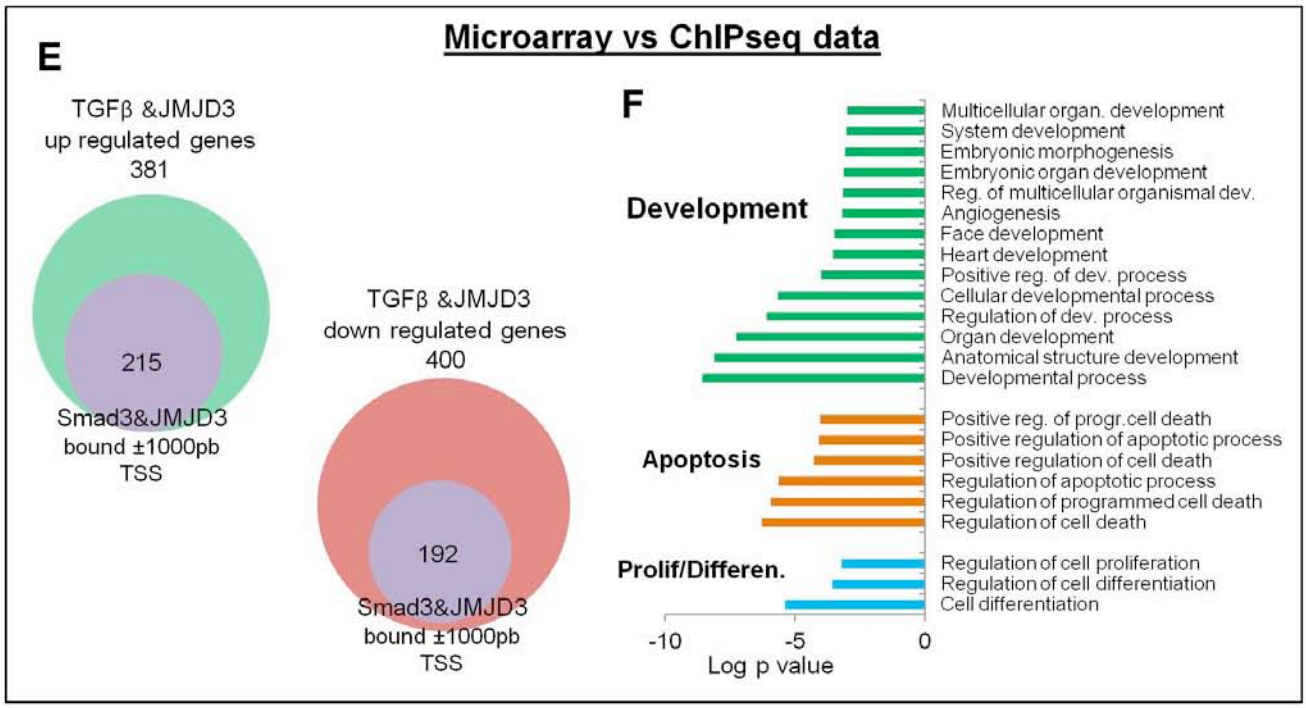
Microarray vs ChIPseq data
E
TGFβ &JMJD3
up regulated genes
381
215
Smad3&JMJD3
bound ±1000pb
TSS
TGFβ &JMJD3
down regulated genes
400
192
Smad3&JMJD3
bound ±1000pb
TSS
F
Development
Multicellular organ. development
System development
Embryonic morphogenesis
Embryonic organ development
Reg. of multicellular organismal dev.
Angiogenesis
Face development
Heart development
Positive reg. of dev. process
Cellular developmental process
Regulation of dev. process
Organ development
Anatomical structure development
Developmental process
Apoptosis
Positive reg. of progr.cell death
Positive regulation of apoptotic process
Positive regulation of cell death
Regulation of apoptotic process
Regulation of programmed cell death
Regulation of cell death
Prolif/Differen.
Regulation of cell proliferation
Regulation of cell differentiation
Cell differentiation
-10
-5
0
Log p value

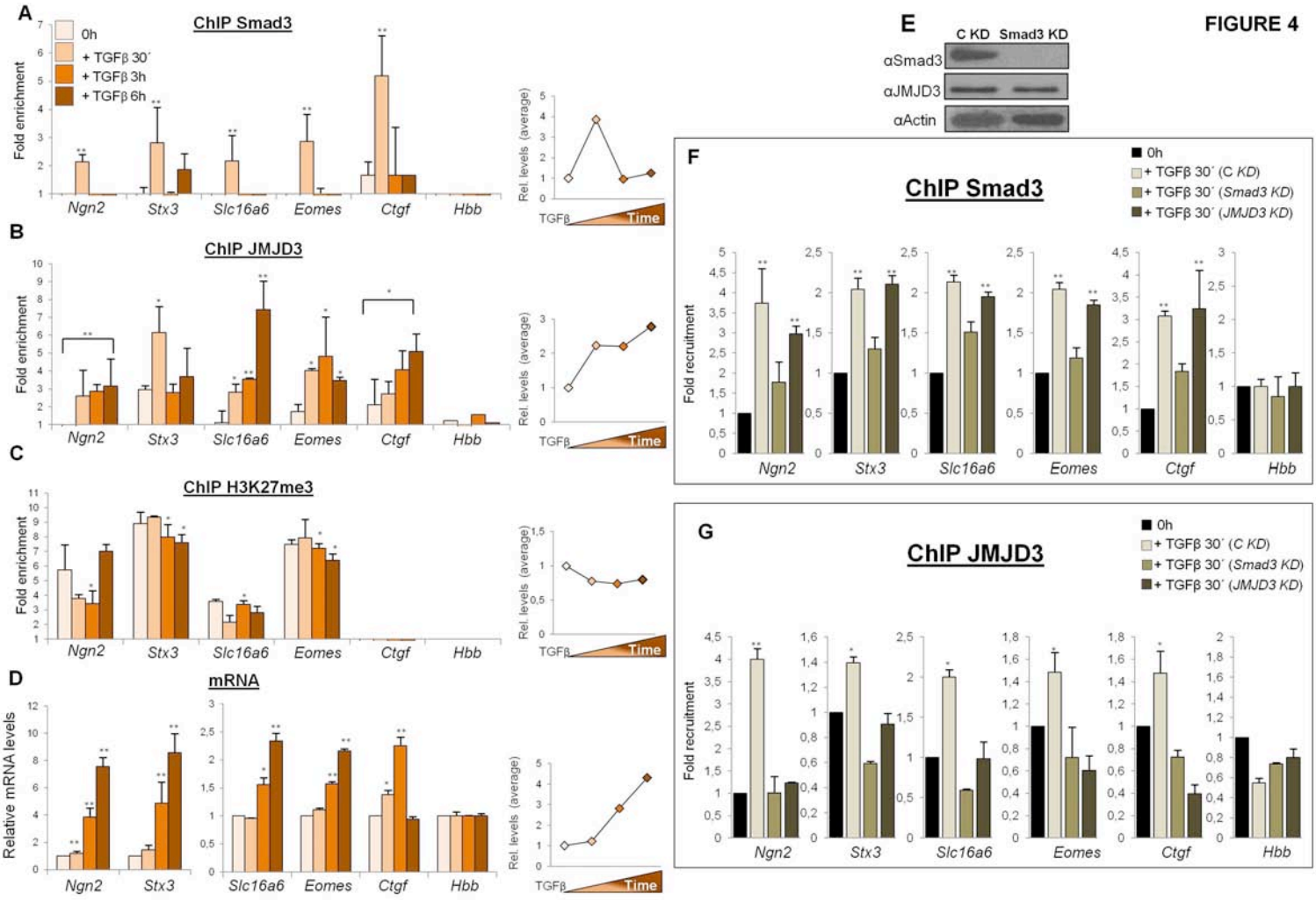
A
ChIP Smad3
0h
+ TGFβ 30´
+ TGFβ 3h
+ TGFβ 6h
Fold enrichment
Ngn2
Stx3
Slc16a6
Eomes
Ctgf
Hbb
Rel. levels (average)
TGFβ
Time
B
ChIP JMJD3
C
ChIP H3K27me3
D
mRNA
Relative mRNA levels
E
C KD
Smad3 KD
αSmad3
αJMJD3
αActin
F
ChIP Smad3
0h
+ TGFβ 30´ (C KD)
+ TGFβ 30´ (Smad3 KD)
+ TGFβ 30´ (JMJD3 KD)
Fold recruitment
G
ChIP JMJD3

FIGURE 4

FIGURE 5

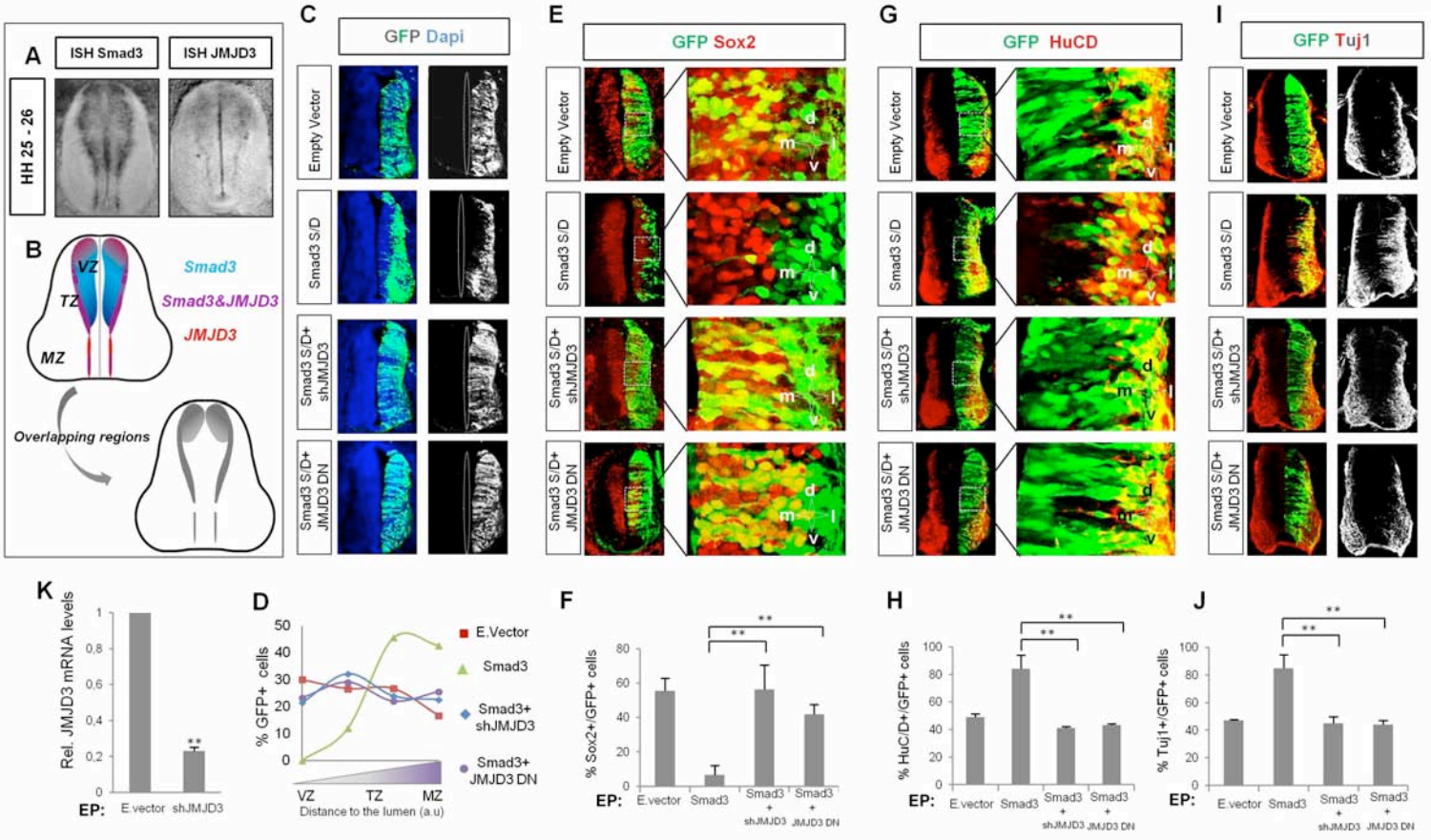
A
ISH Smad3
ISH JMJD3
HH 25 - 26
B
VZ
TZ
MZ
Smad3
Smad3&JMJD3
JMJD3
Overlapping regions
C
GFP Dapi
E
GFP Sox2
G
GFP HuCD
I
GFP Tuj1
Empty Vector
Smad3 S/D
Smad3 S/D+ shJMJD3
Smad3 S/D+ JMJD3 DN
d
m
l
v
K
Rel. JMJD3 mRNA levels
EP:
E.vector
shJMJD3
D
% GFP+ cells
E.Vector
Smad3
Smad3+ shJMJD3
Smad3+ JMJD3 DN
VZ
TZ
MZ
Distance to the lumen (a.u)
F
% Sox2+/GFP+ cells
H
% HuC/D+/GFP+ cells
J
% Tuj1+/GFP+ cells
Smad3
Smad3 + shJMJD3
Smad3 + JMJD3 DN

FIGURE 6

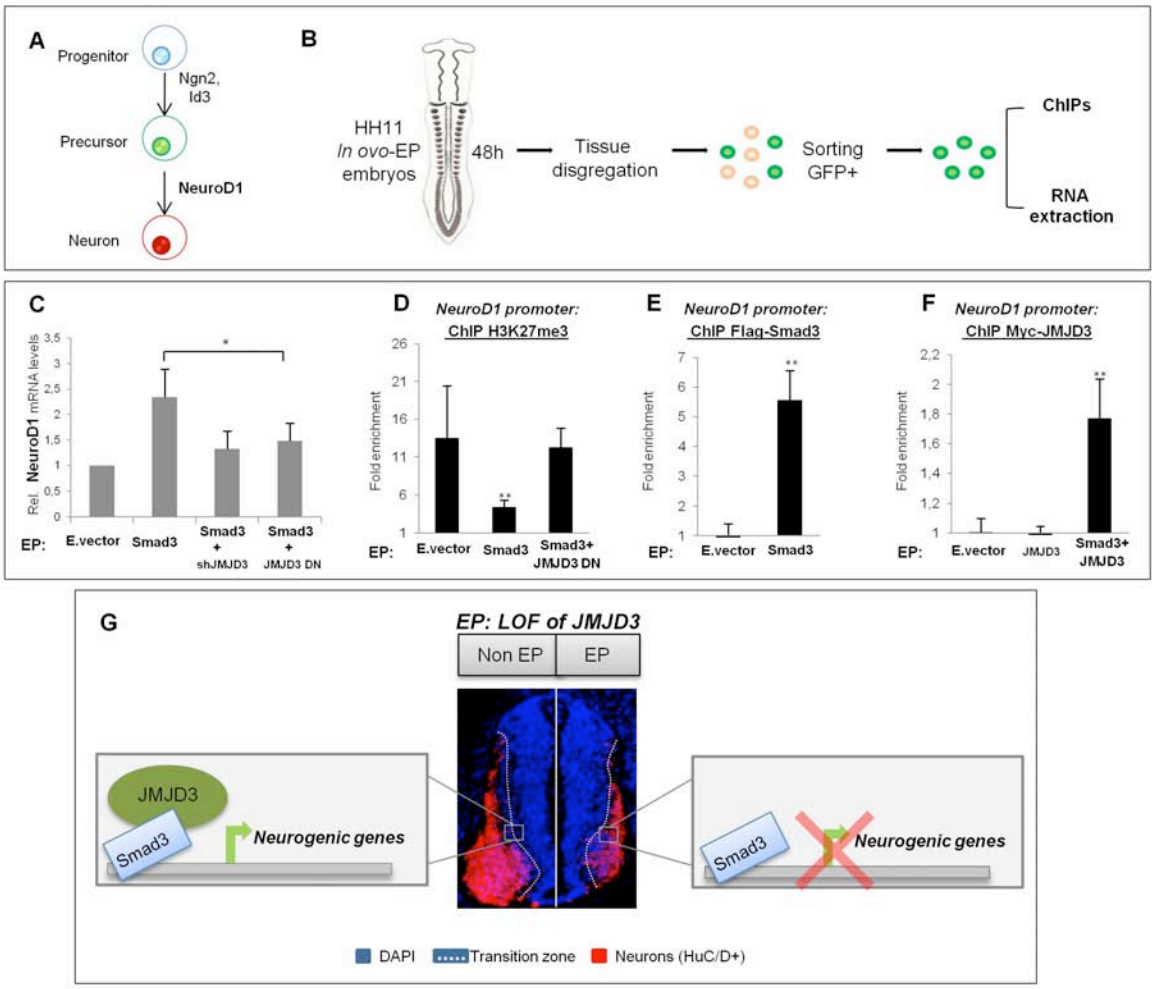
A
Progenitor
Ngn2, Id3
Precursor
NeuroD1
Neuron
B
HH11
In ovo-EP
embryos
48h
Tissue disgregation
Sorting GFP+
ChIPs
RNA extraction
C
Rel. NeuroD1 mRNA levels
EP:
E.vector
Smad3
Smad3 + shJMJD3
Smad3 + JMJD3 DN
D
NeuroD1 promoter:
ChIP H3K27me3
Fold enrichment
E.vector
Smad3
Smad3+ JMJD3 DN
E
NeuroD1 promoter:
ChIP Flag-Smad3
F
NeuroD1 promoter:
ChIP Myc-JMJD3
JMJD3
Smad3+ JMJD3
G
EP: LOF of JMJD3
Non EP
EP
JMJD3
Smad3
Neurogenic genes
DAPI
Transition zone
Neurons (HuC/D+)